



The origin of geothermal waters in Morocco: Multiple isotope tracers for delineating sources of water-rock interactions



Lhoussaine Bouchaou^{a, *}, Nathaniel R. Warner^b, Tarik Tagma^c, Mohammed Hssaisoune^d, Avner Vengosh^{e, *}

^a Ibn Zohr University, Faculty of Sciences, Applied Geology and Geo-Environment Laboratory, Agadir, Morocco

^b Civil & Environmental Engineering, The Pennsylvania State University, University Park, PA, USA

^c Hassan 1st University, Polydisciplinary Faculty of Khouribga, Khouribga, Morocco

^d Sultan Moulay Slimane University, Faculty of Sciences and Techniques, Department of Earth Sciences, Béni Mellal, Morocco

^e Nicholas School of the Environment, Duke University, Durham, NC, USA

ARTICLE INFO

Article history:

Received 31 March 2017

Received in revised form

3 July 2017

Accepted 4 July 2017

Available online 8 July 2017

Handling editor: Elisa Sacchi.

Keywords:

Isotopes

Geochemistry

Geothermal water

Mineralization

Morocco

ABSTRACT

The geochemical and isotopic (strontium, boron, radium, oxygen, hydrogen) variations of geothermal waters from five different regions in Morocco were investigated in order to evaluate the sources of solutes and the mechanisms of water-rock interaction. During 2008 to 2010, twenty-two geothermal water samples were collected from the southern, central, and northern parts of Morocco. The water samples were analyzed for major and trace elements, stable isotopes ($\delta^{18}\text{O}$, $\delta^2\text{H}$) naturally occurring radionuclides (^{226}Ra , ^{228}Ra , ^{224}Ra), and isotopes of dissolved strontium ($^{87}\text{Sr}/^{86}\text{Sr}$) and boron ($\delta^{11}\text{B}$). The Moroccan geothermal waters exhibited a wide range of salinity, ranging from 590 to 25,000 mg/L with predominance of chloride, sodium, sulfate, calcium, and bicarbonate ions. Integration of the geochemical and isotope data suggests that the geothermal waters in Morocco originate from recharge of meteoric water and water-rock interactions. The predominance of chloride and sodium and the relatively low Br/Cl ratios ($<1.5 \times 10^{-3}$), combined with Ca/SO₄ ratios ~ 1 suggest that halite and sulfate (gypsum/anhydrite) minerals are the major rock sources for mineralization of the geothermal waters. The variations of $^{87}\text{Sr}/^{86}\text{Sr}$ ratios (0.7076–0.7122) and $\delta^{11}\text{B}$ (5.3‰–29.3‰) were used to distinguish two rock sources (1) dissolution of marine sulfate/carbonate rocks with Sr isotope composition that correspond to the expected ratios in seawater during time of deposition; and (2) non-marine sources with higher $^{87}\text{Sr}/^{86}\text{Sr}$ and $\delta^{11}\text{B}$, presumably from interactions with clay minerals and shale rocks. The variations of radium isotopes indicate that the alpha-recoil of the parent nuclides on the host rocks caused mobilization of the short-lived ^{224}Ra and ^{228}Ra to the geochemical waters. The low $^{228}\text{Ra}/^{226}\text{Ra}$ ratios (activity ratios of 0.04–0.14) measured in the geothermal waters mimic the Th/U ratios in the source rocks, which indicate predominance of uranium over thorium. Our data show that some of the geothermal waters in Morocco are characterized by high salinity, and in some systems also by elevated radioactivity above international drinking water standards, which limits their utilization for agricultural and domestic applications. Adequate treatment is therefore required to use geothermal waters in Morocco as an alternative or additional water source. Other geothermal waters with low mineralization can be utilized as alternative resource for the agricultural and domestic sectors without any restrictions.

© 2017 Elsevier Ltd. All rights reserved.

1. Introduction

Since early civilization, geothermal water has been utilized for

spiritual, therapeutic, recreation, and agriculture, among other functions. In Morocco, geothermal waters discharge from springs and artesian boreholes and are prevalent in southern, central and

* Corresponding author.

E-mail addresses: l.bouchaou@uiz.ac.ma (L. Bouchaou), nrw6@enr.psu.edu (N.R. Warner), tariktagma@gmail.com (T. Tagma), hsaisoune.med@gmail.com (M. Hssaisoune), vengosh@duke.edu (A. Vengosh).

northern parts of the country (Fig. 1). Some springs are known by their therapeutic purposes for both bathing and consumption (e.g., Moulay Yacoub Fes, Outita, Moulay Idriss, Chafia and Abainou), while other CO₂ rich mineral waters are bottled, and sold commercially as mineral water (e.g., Sidi Hrazem and Oulmes). Previous studies have surveyed the location of geothermal fields through southern, central and northern Morocco (El Morabiti et al., 1998; Lahrach et al., 1998; Zarhloule et al., 1998, 2007; Rimi, 2000; Rimi et al., 1998, 2012; Ettayfi et al., 2012), while others evaluated the chemistry, hydrogeology and isotopic (¹⁸O, ²H, ¹³C, and ¹⁴C) compositions of the groundwater systems (Cidu and Bahaj, 2000; Hakam et al., 2001, 2015; Winkel et al., 2002; Tassi et al., 2006).

In this study we present new geochemical data of twenty-two geothermal water samples collected from southern (Souss Basin and Anti-Atlas Mountains), central (High Atlas and Tadhla Basin), and northern (Rif Mountains) parts of Morocco (Fig. 1). While the previous studies of geothermal waters in Morocco have focused on water sources and residence time using stable and radiocarbon isotopes, here we expand the geochemical toolbox and include isotopes of strontium (⁸⁷Sr/⁸⁶Sr), boron (δ¹¹B), and radium (²²⁶Ra, ²²⁸Ra, ²²⁴Ra) that together with geochemical variations are used to the delineate the sources of solutes in the geochemical water, the mechanism of solute mobilization, and the type of source rocks that control the chemistry of the geothermal waters. In addition to the geochemical study, this paper aims to provide an assessment of the

suitability of Moroccan geothermal water as an alternative water source in areas of high water scarcity.

2. Background and methods

2.1. Sample sources

Geothermal samples were collected from 22 sites between December 2008 and April 2010 to represent a wide geographical range and a broad range of uses. Table 1 summarizes the source type, location, use, geology, and characterization of the Moroccan geochemical waters.

2.2. Analytical methods

Temperature (°C), pH and electrical conductivity (μS/cm) of the waters were determined in the field at the point of discharge. Water samples were collected, field-filtered with 0.45 μm, and preserved in the field. All water samples were shipped to Duke University for analysis of major and trace elements and isotope (O, H, B, Sr, Ra) ratios. Major anions (SO₄, Cl, Br) were determined by ion chromatography (IC) on a Thermo- Fisher Dionex 2100, and major cations (Na, Ca, Mg) were measured by direct current plasma optical emission spectrometry (DCP-OES). Boron and strontium were determined with a VG PlasmaQuad-3 inductively

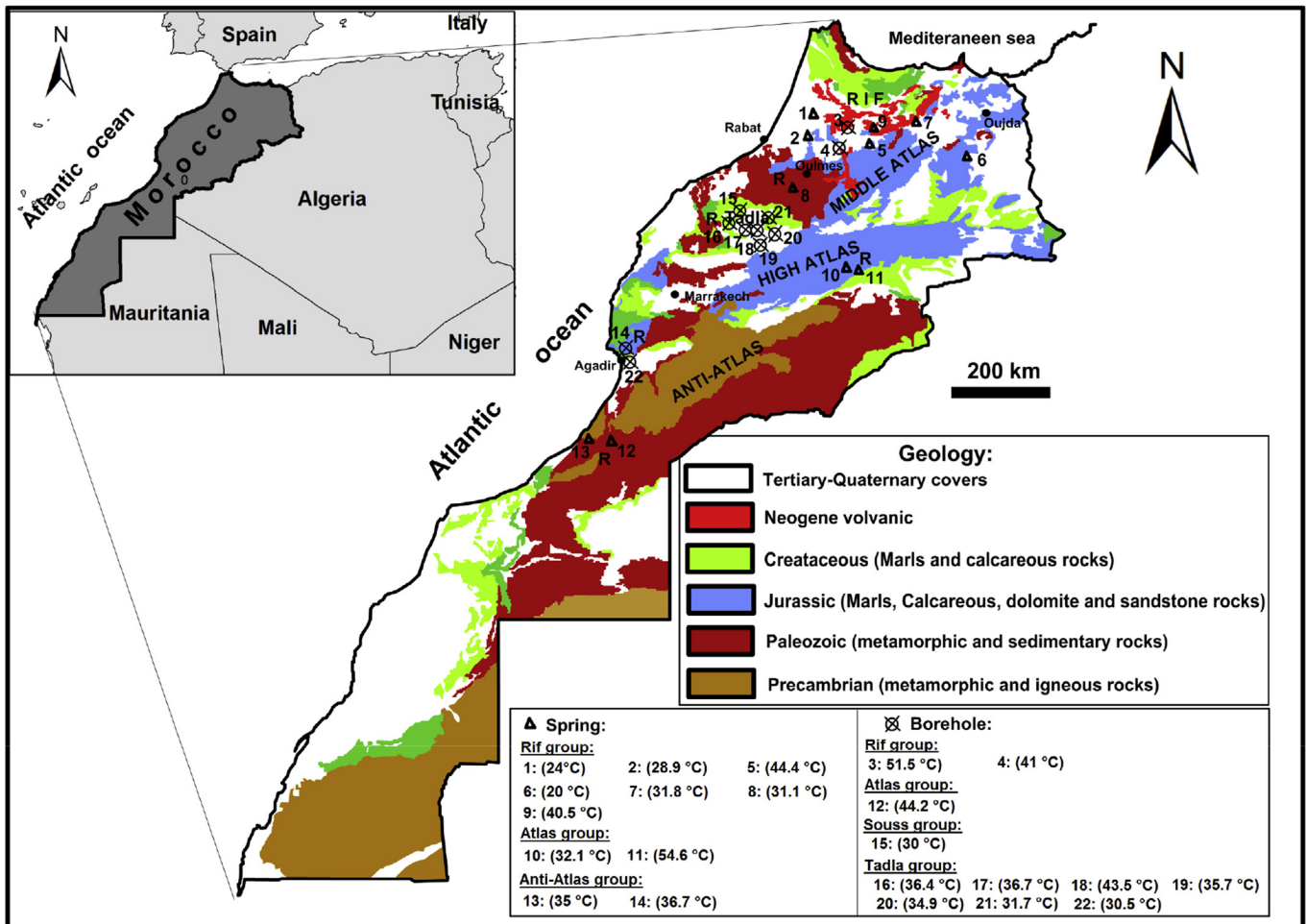


Fig. 1. A geologic map of Morocco with sampling location. Geothermal springs and boreholes investigated in this study are indicated with a triangle and circle, respectively. The legend shows the sample number IDs and the temperature values. Samples were sorted according to their geographical distribution.

Table 1

List of the geothermal waters investigated in this study and background information on the water use, geology and site characteristics.

Sample #	Type	Group	Name & Location	Uses	Geology and characterization
1	S	Rif	My Yacoub in Bab Tiouka; Prerifan Ridge, Mt. Yacoub	SPA	Miocene (Tortonian) carbonate marls. This spring is characterized by high degassing of H ₂ S. Previous studies suggested either deep-water circulation and contact with Triassic evaporite formations, or a contact with halite at the level of the draining fault. (Cidu and Bahaj, 2000)
2	S		Hamma My Driss Zerhou; Prerifan Ridge	SPA and drinking water	Lower Lias formation composed of carbonate and anhydrite minerals
3	B		My Yacoub; Southern Rift Valley	SPA	Tortonian (Miocene) marls. Previous studies have suggested that these waters have been circulated within a carbonate aquifer and have a residence time between 0 and 6000 years BP. (Winckel et al., 2002)
4	B		Ain Allah; Southern Rift Valley	SPA and drinking water	A 1516m borehole composed of (1) Quaternary lacustrine limestone (0–92m); (2) Miocene Grey Marls (92–1316 m); and (3) Liassic Limestone and dolomites (1316–1516m).
5	S		Sidi Chafi	SPA	Triassic gypsum formations, near a contact with Paleocene-Eocene marl, Lias dolomitic and carbonate rocks, anticline, Eastern Morocco.
6	S		Hajra Safra; Eastern Rif Belt	SPA	Triassic gypsum formations, near a contact with Paleocene-Eocene marl. The springs is characterized by high degassing of CO ₂ and H ₂ S
7	S		Hamma Zalagh; Zalagh Mountain, Prerifan ridges	SPA and drinking water (limited use)	Miocene green marls, near E-W fault with Lower Lias dolomite and limestone rocks
8	S	Rif-bottled	Sidi Harazem; Southern Rift Valley	Drinking water	This water is bottled and sold in Moroccan markets. A 270m deep borehole is composed of Upper Miocene marls, sand and bioclastic limestone (0–70m) and Lias limestone and dolomites (70–270m).
9	S		Sidi Harazem; Southern Rift Valley	Drinking water	Granitic rocks characterized by high gaseous mineral water with high bicarbonate
10	S	High Atlas	My Hachem; High Atlas Mountains	SPA and drinking water	Liassic limestone
11	S		My Ali Cherif; Ziz River, High Atlas Mountains	SPA and drinking water (limited use)	Liassic limestone
12	S		Ait Lamine; High Atlas Mountains, north of Agadir	SPA	A 1100 m depth borehole in Cretaceous carbonate and gypsum
13	B	Anti-Atlas	Lalla Mellouka; Anti-Atlas Mountains	SPA and drinking water (limited use)	Lower Cambrian limestone
14	S		Abeinou; Anti-Atlas Mountains	SPA and drinking water (limited use)	Lower Cambrian limestone
15	B	Souss	Kleaa; Souss Plain	Irrigation	A borehole drilled into confined Turonian carbonates. (Bouchaou et al., 2008)
16,17	B	Tadlha	ONEP Drill; Tadla Plain	Drinking water	Both are 390 m deep boreholes drilled into multiple aquifers of Turonian Carbonate that lie underneath the Tadla Plain.
18,19	B		Artesian; Tadla Plain	Irrigation and drinking water	Both are 400 m deep boreholes drilled into multiple aquifers of Turonian Carbonate that lie underneath the Tadla Plain.
20,21,22	B		ONEP Drill; Tadla Plain	Drinking water	All 3 are boreholes drilled through multilayer aquifers of Eocene and Turonian carbonates beneath the Tadla Plain.

coupled plasma mass-spectrometer (ICP-MS). Sample signals/concentrations were bounded by matrix standards and reproducibility was compared to external standards. Error in reproducibility of external standards was less than 5%. Total alkalinity was determined in duplicate by titration with HCl to pH 4.5. Stable isotopes were determined by continuous flow isotope ratio mass spectrometry (TCEA-CFIRMS), using a ThermoFinnigan TCEA and Delta + XL mass spectrometer at the Duke Environmental Isotope Laboratory (DEVIL). Analytical precisions for $\delta^{18}\text{O}$ and $\delta^2\text{H}$ were estimated as $\pm 0.1\%$ and $\pm 1.5\%$, respectively. Replicate measurements of $\delta^{18}\text{O}$ and $\delta^2\text{H}$ were also performed by spectrometry using a Picarro L2120 at the Applied Geology and Geo-Environment Laboratory, Ibn Zohr University, Agadir, Morocco. Strontium and boron isotopes were determined by thermal ionization mass spectrometry (TIMS) using a ThermoFisher Triton. The average $^{87}\text{Sr}/^{86}\text{Sr}$ of the SRM-987 standard measured during this study was 0.710266 ± 0.000005 (SD). The SD for $^{87}\text{Sr}/^{86}\text{Sr}$ on duplicate samples was ± 0.000008 . The average $^{11}\text{B}/^{10}\text{B}$ of NBS 951 boric acid standard measured during this study was 4.0061 ± 0.0005 (SD). Boron isotopes were measured in negative ionization mode (NTIMS) with an artificial seawater load solution (Dwyer and Vengosh, 2008). Boron measurements are presented in standard notation ($\delta^{11}\text{B}$) relative to the 951 standard. The SD of duplicate groundwater samples in this study was ± 0.0012 leading to a SD in $\delta^{11}\text{B}$ notation of $\pm 0.3\%$. Radium isotopes (^{224}Ra , ^{226}Ra and ^{228}Ra) were analyzed at the Duke University Laboratory for Environmental Analysis of Radio Nuclides (LEARN).

2.3. Geologic and hydrologic settings

The geology of Morocco is complex with formations that range from Precambrian to Quaternary in age. For simplicity, we divide the geologic formations into six units based on age, Precambrian, Paleozoic, Jurassic, Cretaceous, Neogene, and Tertiary-Quaternary (Fig. 1). The Precambrian is localized mainly in southern Morocco and composed of igneous granites and metamorphic rocks within the Anti-Atlas Mountains. Overlying the Precambrian basement are Paleozoic-age formations also largely in the Anti-Atlas Mountains Morocco but also as in central part of Morocco in High Atlas Mountains. The Paleozoic-age formations are generally metamorphic and sedimentary.

Triassic and Jurassic age sandstones, limestone and evaporite deposits are abundant in the High and Middle Atlas Mountains. During the Late Cretaceous there was a general transgression and return to shallow marine conditions in the Atlas and the northern Saharan regions. The Cretaceous-age units contain fluvial sandstones, marls and conglomerates. Paleocene-Eocene thin sandy to marl sediments overlie unconformably the Late Cretaceous strata. Neogene volcanic rocks are found mainly in northern Morocco with occasional intrusive basalts from rift-related magmatism. The youngest rocks, the Quaternary to Tertiary, are composed mainly by alluvial sands, gravels, and lacustrine limestone. These thick alluvial and coastal deposits form major basins, including the Souss Basin in southern Morocco near Agadir; the Tadlha Basin around Marrakech in central Morocco; and several basins along the

Atlantic Coast and from Rabat to Oujda (Fig. 1).

The Rif region in northern Morocco is a complex zone that includes significant volumes of Cretaceous and Tertiary limestone, as well as slivers of older rocks, including ophiolites and metamorphic basement. The Rif is a thrust zone, part of the Alpine orogenic zone that has caused complex layering of sedimentary formations, and mountainous areas. Other major Cretaceous to Tertiary basins include the Plateau des Phosphates north of Marrakech, which includes limestone and marls; and the Haut Plateau in the northeast of Morocco, which includes calcareous lacustrine deposits.

Precipitation in the High, Middle and Anti Atlas Mountains is the major source of Morocco's water resources. Snowmelt and rain feed productive aquifer formations in most of the major sedimentary units, at various depths including karst aquifers that are found mainly in the Rif and the High, Middle and Anti Atlas Mountains. Given the complex geology, including several thrust regions, geothermal water is often associated with spring systems boreholes that have been drilled near fault zones.

3. Results

3.1. Chemical characterization

The geothermal water samples showed wide ranges in salinity (TDS from 588 mg/L to 25,000 mg/L), temperature (24 °C to 54.4 °C), and pH (6.02–7.45; Table 2). The lowest pH measurements were obtained in CO₂ rich springs (#3,9). Major element chemistry reveals three major water groups (Fig. 2): (1) Na-Cl water type with the highest TDS (#1, 3, 5, 6, 11 and 12); (2) Ca-SO₄ water type (#2, 12, 13, and 14); and (3) Ca-Mg-HCO₃ water type, with lower salinity (#4, 9, and 15 through 22).

The variations of major elements of chloride, sodium, calcium, magnesium, bicarbonate and sulfate with TDS (Fig. 2) show that chloride and sodium are the major constituents that generate the overall salinity, followed by sulfate, calcium, and magnesium. Bicarbonate concentrations were typically low (<600 mg/L) and were not correlated with TDS; in only one geothermal system from granitic rocks (#9), the bicarbonate levels were high (1000 mg/L). In most geothermal waters the sulfate was associated with the TDS, except the most saline site (#3) with low sulfate contents (Fig. 2). Minor elements of boron and strontium also showed high correlations with the overall TDS (Fig. 2).

3.2. Isotopic characterization

The stable isotopes of δ¹⁸O and δ²H in the geothermal water ranged from - 8.7‰ to -4.5‰ and from -60.1‰ to -32.2‰ V-SMOW, respectively (Fig. 3). The δ²H-δ¹⁸O variations were compared to the Global Meteoric Water Line (GMWL; δ²H = 8*δ¹⁸O + 10; Craig, 1961; Dansgaard, 1964) and to the local meteoric water line in Morocco (δ²H = 8*δ¹⁸O + 14; Fig. 3), which represents the local precipitation (Bouchaou et al., 2013; Raibi et al., 2006; Ouda et al., 2004). The δ¹⁸O and δ²H values of the geothermal waters vary along the meteoric water line and not ¹⁸O-enrichment from high-temperature water-rock interactions was observed. Likewise, no correlations have been observed between the stable isotopes ratios of oxygen and hydrogen and chloride concentrations or Br/Cl ratio. The lack of correlations with salinity and the similarly to the meteoric line therefore indicate ground-water recharge without extensive evaporation or influence of external saline water. Deuterium excess values (d-excess) ranged from 4‰ to 20‰ (Table 2), with most values higher than 10‰. As the air masses in Morocco originate mainly from the Atlantic Ocean, the relatively high deuterium excess values suggest

Table 2 Major and trace elements, combined with stable isotopes (oxygen, hydrogen, boron, and strontium) and radium isotopes data of Moroccan geothermal waters. ND indicates the analysis was not determined, while BDL is below detection limit.

Sample	pH	E.C. μS/cm	Temp °C	Cl mg/L	SO ₄ mg/L	NO ₃ mg/L	HCO ₃ mg/L	Br mg/L	Ca mg/L	Mg mg/L	Na mg/L	Sr mg/L	B mg/L	Li mg/L	U mg/L	TDS (mg/L)	Ra-224 Bq/L	Ra-228 Bq/L	Ra-226 Bq/L	⁸⁷ Sr/ ⁸⁶ Sr ratio	δ ¹¹ B (‰)	δ ¹⁸ O (‰)	δ ² H (‰)	² H excess
1	7.1	21,800	24	7052	301	0.4	560	19.5	432	250	4071	22.1	9.82	9.4	0.77	12,731	ND	ND	0.02	0.708927	25.4	-4.5	-32.2	3.8
2	6.8	3330	29	395	1153	2.2	280	0.98	373	84	238	5.3	0.19	7.2	0.17	2540	0.02	0.03	0.23	0.707739	9.5	-5.8	-33.6	12.8
3	6.3	44,000	52	17258	16	0.5	270	30.0	1311	346	5642	69.2	7.46	16.4	0.02	25,034	ND	ND	0.05	0.711633	19.8	6.2	-40.3	9.3
4	7.1	790	41	82	25	5.7	325	0.29	59	31	53	0.2	0.02	6.6	0.67	594	BDL	BDL	0.03	0.710029	ND	6.1	-42.2	6.6
5	6.7	13,920	44	3810	2012	0.9	ND	2.81	795	183	2640	14.5	0.30	17.4	0.48	9478	0.01	BDL	0.01	0.708048	7.9	8.7	-58.6	11
6	6.9	25,500	20	7144	3026	0.4	500	2.65	1004	147	4555	14.4	2.37	7.5	0.52	16,405	nd	BDL	0.00	0.708322	ND	6.8	-49	5.4
7	7.3	7300	32	2146	177	0.2	251	2.98	177	55	1362	3.9	0.51	9.5	BDL	4187	0.03	0.06	0.12	0.712228	19.5	6.6	-35.6	16.9
8	7.2	1368	33	321	22	3.7	340	0.76	79	42	177	0.7	0.04	7.4	0.34	996	0.01	0.01	0.05	0.711917	29.3	6.8	-42.9	11.5
9	6.0	2290	41	266	11	0.6	1030	1.87	173	51	236	0.7	0.47	67.5	BDL	1850	0.02	0.03	0.81	0.723293	7.9	7	-36.1	19.9
10	7.4	2420	32	561	93	5.7	259	0.18	82	24	356	2.1	0.05	ND	ND	1382	0.01	0.01	0.04	0.708327	16.0	8.3	-60.1	6.3
11	6.4	22,000	55	4134	1584	2.7	256	0.7	529	84	2527	21.9	0.18	ND	ND	9139	0.28	0.28	1.70	0.70814	5.3	ND	ND	ND
12	7.1	3200	44	84	1912	1.1	244	0.07	502	146	132	10.2	0.67	11.8	BDL	3046	0.12	0.08	0.25	0.707604	ND	5.3	-25.4	17
13	7.8	2850	35	39	1576	2.7	220	0.07	530	86	51	8.8	0.05	17.1	BDL	2552	ND	0.17	0.73	0.708905	16.8	7.6	-53.4	7.6
14	6.9	3470	37	265	1503	1.3	244	0.08	548	88	211	13.7	0.06	14.8	BDL	2910	ND	0.15	0.66	0.708979	13.2	5.3	-34.1	8.5
15	7.0	1976	30	238	375	0.3	437	0.56	103	122	136	3.6	ND	ND	ND	1416	ND	ND	ND	0.707659	12.0	4.9	-34.3	4.9
16	7.1	1585	36	147	168	5	293	0.28	108	39	82	0.6	0.02	7.0	0.41	851	0.01	0.01	0.08	ND	ND	6.3	-40.5	10
17	7.2	1109	37	134	63	5.7	299	0.26	84	35	77	0.3	0.02	6.9	0.58	708	0.01	0.01	0.09	0.708655	ND	6.9	-41.7	13.2
18	7.0	1687	44	264	240	1.7	275	0.52	138	40	138	0.9	0.05	10.1	1.22	1110	0.02	0.01	0.17	0.708159	ND	7.7	-43.8	17.4
19	7.2	836	36	41	133	0.3	275	0.12	83	35	30	1.7	0.10	ND	BDL	600	0.02	0.01	0.20	0.707903	ND	7.1	-40.4	16.1
20	7.2	1085	35	115	110	0.9	267	0.18	77	34	83	0.8	0.04	ND	2.7	693	ND	0.01	0.21	ND	ND	7.2	-39.4	18
21	7.5	1093	32	148	55	2	287	0.13	71	34	94	0.6	0.03	10.6	2.96	707	ND	0.02	0.25	0.707976	ND	-6.6	-39.9	12.5
22	7.2	1012	31	129	43	2.6	311	0.08	68	33	85	0.5	0.02	10.7	2.49	687	ND	ND	ND	ND	ND	-6.6	-40.7	11.9

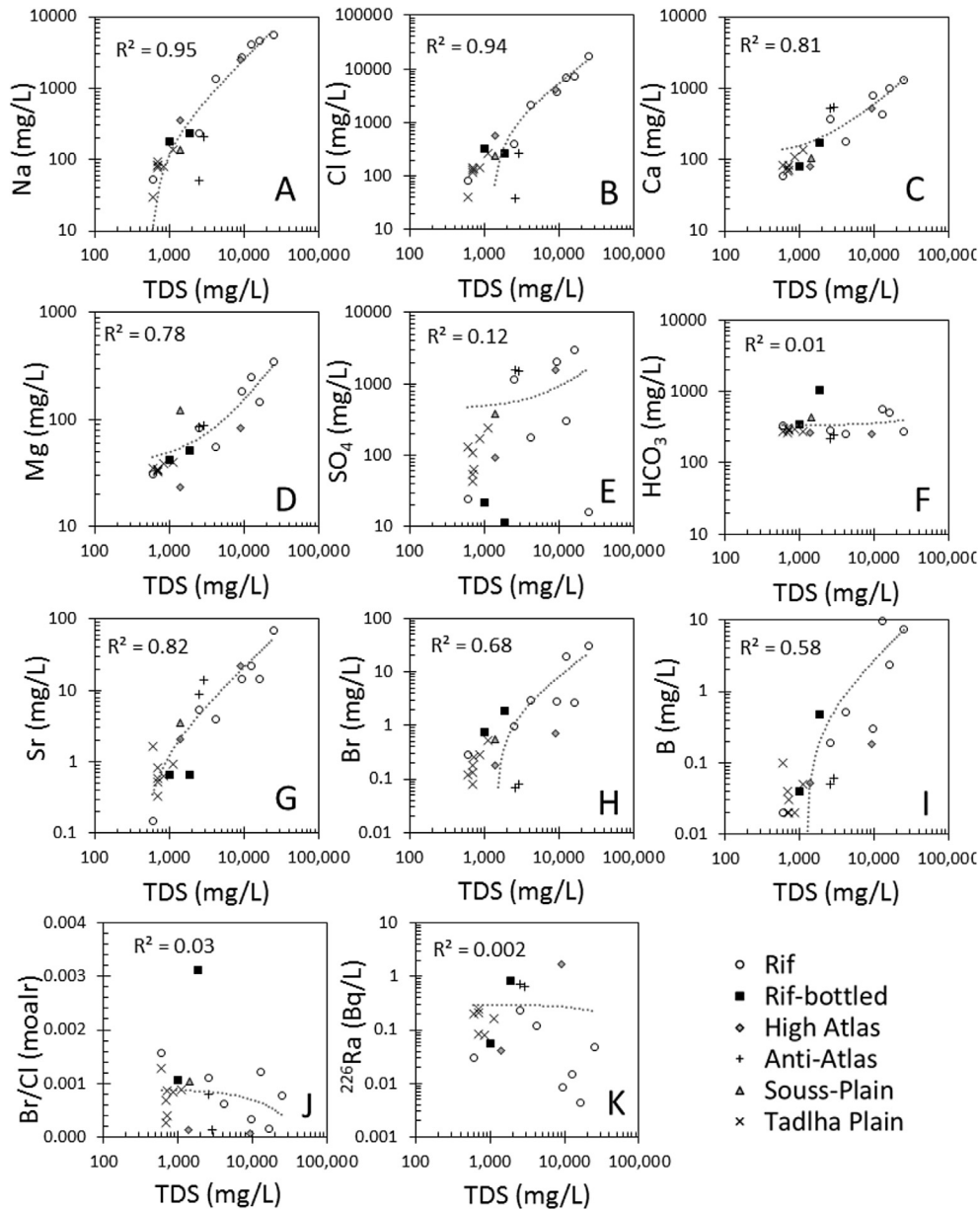


Fig. 2. Variations of sodium (A), chloride (B), calcium (C), magnesium (D), sulfate (E), bicarbonate (F), strontium (G), bromide (H), boron (I), Br/Cl (J), and ^{226}Ra (K) with TDS in the geothermal waters in Morocco. All concentrations are in mg/L, except for ^{226}Ra , which is reported in Bq/L. Note the high correlations with statistical significance (i.e., high R^2 values and p values < 0.001) for chloride, sodium, calcium, magnesium, strontium, and boron with TDS, while sulfate and bicarbonate were not always correlated with TDS.

significant contributions of moisture from a secondary origin such as the Mediterranean Sea or local vapor flux through evaporation to rainfall (Clark and Fritz, 1997). The samples showing high deuterium excess (#7, 9, 12, 18, 19, and 20) can be also explained by recharge from high altitude (Bouchaou et al., 2009). A similar process has been highlighted in other regions not influenced by the Mediterranean air masses (Sosa et al., 2011).

Strontium isotopic ratios ($^{87}\text{Sr}/^{86}\text{Sr}$) varied among geothermal waters from carbonate rocks from 0.7077 (#15; sourced from Cretaceous limestone in Souss area) to 0.7122 (#7; sourced from Miocene marls in Zalagh Mountain). A single geothermal sample from the granitic area of Oulmes yielded much higher radiogenic ratio of 0.7230 (9; Fig. 3). Boron isotopic ratios varied among geothermal waters from carbonate rocks from $\delta^{11}\text{B}$ of 5.3‰ (11; Liassic limestone at High Atlas Mountain) to 29.3‰ (8; Lias

limestone and dolomites at Southern rift Valley Miocene marls in Zalagh Mountain). A single geothermal sample from a granitic area of Oulmes yielded low $\delta^{11}\text{B}$ of 7.9‰ (9; Fig. 3). The high saline water with high boron concentrations (1, 3) had also relatively high $\delta^{11}\text{B}$ of 19.8‰ and 25.5‰ (Fig. 3).

The long-lived radium nuclides of ^{228}Ra and ^{226}Ra showed large variations in ^{226}Ra , between 0.003 Bq/L (#6) to 1.69 Bq/L (#11). The highest ^{226}Ra levels were observed in both the High Atlas Mountains (#11: 1.69 Bq/L) and the Anti-Atlas Mountains (#13: 0.72 Bq/L and #14: 0.65 Bq/L; Fig. 4). The ^{228}Ra levels were systematically lower than those of ^{226}Ra , and the data show $^{228}\text{Ra}/^{226}\text{Ra}$ activity ratios distribution along two lines: (1) higher $^{228}\text{Ra}/^{226}\text{Ra}$ activity ratios of 0.14 for geothermal waters from carbonate and marls rocks from the Rif area; and (2) lower $^{228}\text{Ra}/^{226}\text{Ra}$ activity ratios of 0.04 for geothermal water from the Atlas Mountain and one sample

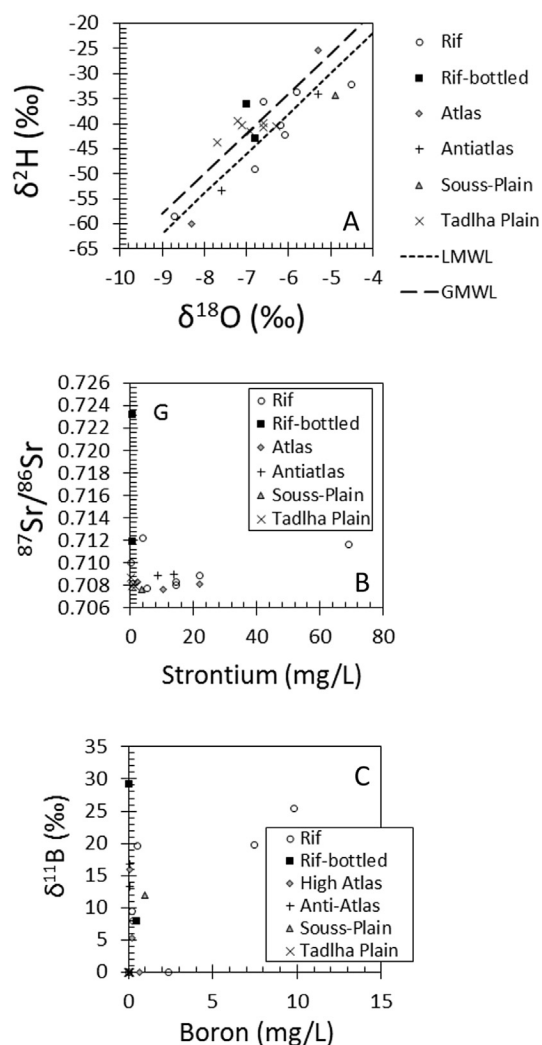


Fig. 3. Variations of oxygen, hydrogen (A), strontium (B), and boron isotopes (C). The upper plot show $\delta^2\text{H}$ versus $\delta^{18}\text{O}$ values as compared to the Global Meteoric Water Line and the local Moroccan Meteoric Water Line. The similarity to the water meteoric water lines suggest that the geothermal waters originated from recharge of meteoric water and water-rock interaction has not modified the stable isotope composition. The middle plot (B) represents $^{87}\text{Sr}/^{86}\text{Sr}$ ratios versus strontium concentrations. The single symsple from a granitic area (#9) from Oulmes District in Central Massif is marked with the letter G. Note the high radiogenic $^{87}\text{Sr}/^{86}\text{Sr}$ ratios of the geothermal water from the granitic area relative to the sites that flow from carbonate/sulfate rocks with much lower $^{87}\text{Sr}/^{86}\text{Sr}$ ratios. The bottom plot (C) represents $\delta^{11}\text{B}$ versus boron concentrations. The large $\delta^{11}\text{B}$ variations were not correlated with boron concentrations.

from the granitic rock (Fig. 4). Although the temperature and TDS of some geothermal systems show correlations, most saline and higher temperature systems (e.g., 3) showed lower ^{226}Ra activities (Fig. 2K). The variations of the short-lived ^{224}Ra were directly correlated to ^{228}Ra with $^{224}\text{Ra}/^{228}\text{Ra}$ activity ratios ~ 1 (Fig. 4).

4. Discussion

4.1. Sources of solutes in the moroccan geothermal waters

All of the waters sampled in this study are saturated with respect to calcite and dolomite, while the majority are undersaturated with respect to gypsum and anhydrite, with the exception of five samples (#6, 11, 12, 13, 14). All samples show ionic balance $\leq 5\%$ except #3 with 18%. This error may be because K was not measured during this study.

While the majority of geothermal waters investigated in this study were collected from systems composed of carbonate rocks, the distribution of major elements in the geothermal waters indicates that the dissolved solutes originated from dissolution of halite and sulfate minerals. The predominance of chloride and sodium, combined with typically low Br/Cl ratios (below the seawater ratio of 1.5×10^{-3} ; Fig. 2j) indicates that halite dissolution is the principle source of the salinity in the Moroccan geothermal waters. Likewise, the association of Ca and sulfate with Ca/SO₄ ratios close to unity (Fig. 5), suggests that the high sulfate and calcium contents of the geothermal waters originated from gypsum dissolution. Combined, the geochemical data suggest that water-rock interactions caused dissolution of evaporite rocks rather than carbonate rocks. In most of the geothermal systems, the bicarbonate levels were low (200–500 mg/L) relative to other constituents derived from halite dissolution such as Na and Cl (Fig. 2). The carbonate levels reflect the equilibrium between carbonate rock dissolution and carbonate coprecipitation into secondary carbonate minerals. The only exception is the geothermal water from the granitic area of Oulmes (#9), where the bicarbonate content was very high (1000 mg/L), reflecting intensive water-rock interactions with silicate minerals, which is common for geothermal waters from silicate rocks systems (Nicholson, 1993; Favara et al., 2001; Vengosh et al., 2002; Carreira et al., 2008; Marques et al., 2006, 2012; Dupalova et al., 2012; Loges et al., 2012).

In addition, the majority of geothermal water samples had $\delta^{18}\text{O}$ and $\delta^2\text{H}$ values that plot near the GMWL and LMWL (Fig. 3A), without indications of evaporation or water-rock interactions (i.e., enrichment of ^{18}O). This suggests that the geothermal waters originated from meteoric water that was recharged to the subsurface through permeable media without secondary surface evaporation. The majority of geothermal samples were collected at high altitude or near the faulted mountain zones, which explains the relative depleted values of ^{18}O and ^2H in some of the geothermal waters. The four samples located above the LMWL (#12, 18, 19, 20) were collected from deeper aquifers within the Tadhla and Souss plains. This supports the hypothesis that the water originated from the high Atlas Mountains, which was highlighted in previous studies (Bouchaou et al., 2009; Winckel et al., 2002; N'da et al., 2016; Penna et al., 2014). Consequently, the data suggest that the geothermal waters in Morocco originated from common meteoric water that recharged to the subsurface and interacted with evaporite rocks composed of halite and sulfate minerals.

In addition to the major elements, we use the strontium and boron isotope variations provide further information on the rock types that control the geothermal water chemistry. The different geological formations in Morocco (Fig. 1) had distinctive $^{87}\text{Sr}/^{86}\text{Sr}$ ratios of several geological units that include: (1) the underlying Precambrian crystalline (granitic and metamorphic rocks) basement with radiogenic $^{87}\text{Sr}/^{86}\text{Sr}$ (>0.712); (2) marine carbonate and/or sulfate (anhydrite) rocks with $^{87}\text{Sr}/^{86}\text{Sr}$ variations that represents the seawater secular Sr isotope ratios during the Paleozoic, Triassic, Jurassic, Cretaceous, and Miocene; and (3) the overlying Middle–Upper Cambrian schist rocks with expected radiogenic $^{87}\text{Sr}/^{86}\text{Sr}$ (>0.710). The Sr isotope ratios of barites in Paleozoic rocks were measured and ranged from 0.71077 to 0.71714 (Castorina et al., 1999). The radiogenic ratios were attributed to leaching of pre-Hercynian schist rocks during the Hercynian orogenesis. As shown in Fig. 3B, the $^{87}\text{Sr}/^{86}\text{Sr}$ ratios of the geothermal water from carbonate and sulfate rocks varied from 0.7077 to 0.71222, while a single sample from the granitic area of Oulmes yielded much higher radiogenic ratio of 0.7230 (#9; Fig. 3B). The high radiogenic $^{87}\text{Sr}/^{86}\text{Sr}$ ratios in Oulmes water are associated with high bicarbonate concentrations (1000 mg/L) and Na/Cl ratio (>1), which are consistent with the composition expected from silicate rocks

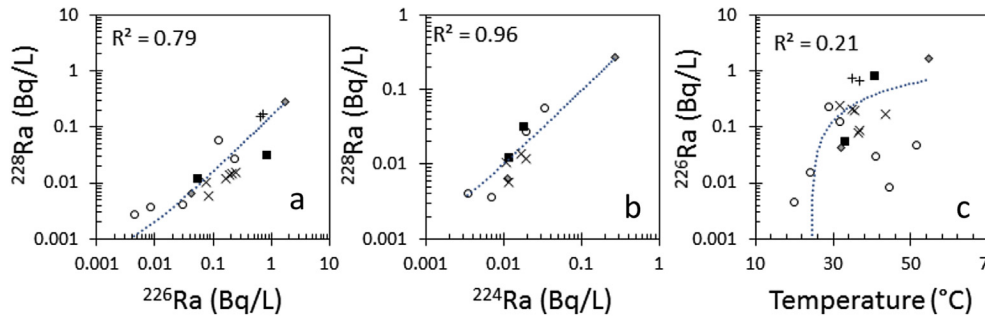


Fig. 4. Variations of radium (^{228}Ra , ^{226}Ra , ^{224}Ra) nuclides activities (concentrations); (a) ^{228}Ra vs ^{226}Ra , (b) ^{228}Ra vs ^{224}Ra , and (c) ^{226}Ra vs Temperature. The $^{228}\text{Ra}/^{226}\text{Ra}$ activity ratios were low (<0.14). The short-lived ^{224}Ra activities were consistent with ^{228}Ra , with $^{228}\text{Ra}/^{224}\text{Ra}$ activity ratios of ~ 1 . The ^{226}Ra variations were not controlled by the temperature of the geothermal waters. These variations suggest that Ra mobilization is controlled by alpha-recoil process from host rocks with predominance of uranium relative to thorium in the source rocks.

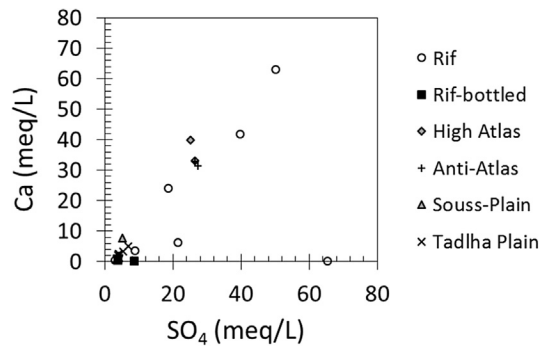


Fig. 5. Calcium versus sulfate (in milliequivalent per liter) of geothermal waters from Morocco, sorted by their location (see Fig. 1). The high correlation between calcium and sulfate and the Ca/SO₄ ratio \sim unity suggest that dissolution of sulfate (gypsum) minerals is the major source of mineralization of the geothermal waters.

dissolution.

In order to further examine the relationships between the $^{87}\text{Sr}/^{86}\text{Sr}$ in the geothermal water and the rock sources, we sorted out the geothermal water samples based on the system lithology. Our sample collected includes five rock types (1) Cambrian Paleozoic (#13–14); (2) Liassic (Jurassic – #2, 4, 5, 8, 10 and 11); (3) Turonian (Late Cretaceous – #12,15, 16, 17., 20–22); (4) Senonian (Late Cretaceous – #18, 19); and (5) Miocene-Neogene (#1, 3, 7). The variations of $^{87}\text{Sr}/^{86}\text{Sr}$ from these five lithological groups are presented in Fig. 6 and compared to the $^{87}\text{Sr}/^{86}\text{Sr}$ ratio of seawater of the specific time of deposition, based on the secular $^{87}\text{Sr}/^{86}\text{Sr}$ variation of seawater with geological time (Burke et al., 1982; Veizer, 1989). The geothermal waters associated with Cambrian rocks had slightly lower $^{87}\text{Sr}/^{86}\text{Sr}$ ratios relative to the expected seawater ratio during the Cambrian (Fig. 6). In contrast, in the other systems we show systematic higher $^{87}\text{Sr}/^{86}\text{Sr}$ ratios relative to the expected seawater curve (Fig. 6). This is particularly shown in the geothermal water from Miocene rocks with much higher $^{87}\text{Sr}/^{86}\text{Sr}$ ratios that the expected seawater ratio during the Miocene. This indicates that the carbonate and sulfate rocks are not the sole sources for strontium, and other rock sources, such as clays and shale with typically high Rb and radiogenic $^{87}\text{Sr}/^{86}\text{Sr}$ are contributing to the geothermal waters.

The $\delta^{11}\text{B}$ values of the geothermal waters varied from 5.3‰ to 29.3‰, without any correlations with the boron content (Fig. 3C). In the case of the geothermal system from the granitic area of Oulmes, the $\delta^{11}\text{B}$ of 7.9‰ could correspond to the granitic rocks composition. For the other geothermal systems, we show that geothermal waters with low $^{87}\text{Sr}/^{86}\text{Sr}$ ratios, which reflect predominance of

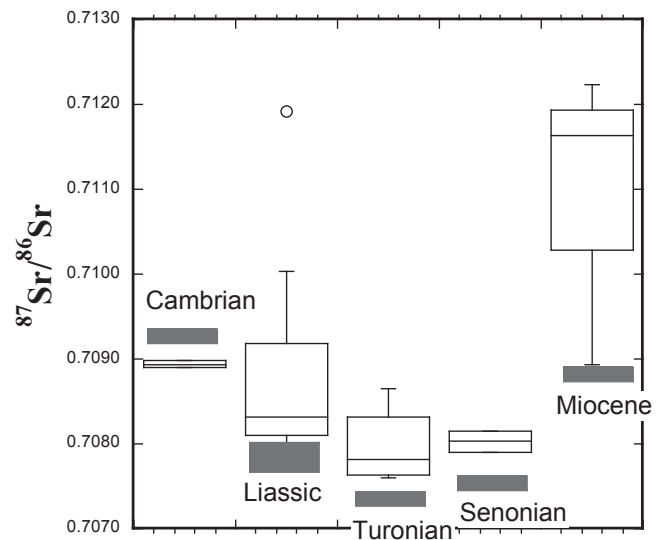


Fig. 6. Box plots of $^{87}\text{Sr}/^{86}\text{Sr}$ variations of the Moroccan geothermal waters sorted by the geology and lithology of the host rocks. In each rock formation the $^{87}\text{Sr}/^{86}\text{Sr}$ variations were compared to the $^{87}\text{Sr}/^{86}\text{Sr}$ value expected for seawater during time of deposition based on the secular $^{87}\text{Sr}/^{86}\text{Sr}$ variations of seawater with time (Burke et al., 1982; Veizer, 1989). The data show that in most cases the $^{87}\text{Sr}/^{86}\text{Sr}$ of the geothermal waters were higher than the ratios expected for seawater during time of formation.

carbonate and sulfate rocks contribution, the $\delta^{11}\text{B}$ values are typically low (5‰–17‰; Fig. 3C), which is consistent with the composition expected from dissolution of marine carbonate and sulfate minerals (Vengosh et al., 1991). Some geothermal waters with higher $^{87}\text{Sr}/^{86}\text{Sr}$ ratios also have higher $\delta^{11}\text{B}$ values (19.5‰–29.3‰; Table 2). The higher $\delta^{11}\text{B}$ values in the latter case could be result from further modification of boron through adsorption processes, in which ^{10}B is selectively retained to clay minerals while the residual groundwater becomes enriched in ^{11}B . Alternatively, the relatively higher $\delta^{11}\text{B}$ values could reflect mobilization of boron from desorption sites on marine clay minerals, which are characterized by $\delta^{11}\text{B}$ –20–30‰ (Vengosh et al., 1991, 1994).

Another way to evaluate the solute sources in the geothermal water is through the correlation between $^{87}\text{Sr}/^{86}\text{Sr}$ and Ca/SO₄ ratios. The data show (Fig. 7) that geothermal waters with Ca/SO₄ \sim unity have typically low $^{87}\text{Sr}/^{86}\text{Sr}$ that correspond to dissolution of marine sulfate minerals with Sr isotope composition that correspond to the ratio in seawater during time of sulfate deposition. On contrast, the rise of the Ca/SO₄ ratios is associated with higher $^{87}\text{Sr}/^{86}\text{Sr}$ ratios, inferring contribution of Sr and Ca from

other rock sources. We propose that desorption of Sr from marine clay minerals would also generate radiogenic (higher) $^{87}\text{Sr}/^{86}\text{Sr}$ ratios in the water given the typically high potassium, and thus ^{87}Rb in clay minerals. Consequently the association of relatively higher $\delta^{11}\text{B}$, $^{87}\text{Sr}/^{86}\text{Sr}$ and Ca/SO_4 ratios (Fig. 7) could reflect the net contribution of marine clay minerals, which are different from the marine sulfate with lower $\delta^{11}\text{B}$ and $^{87}\text{Sr}/^{86}\text{Sr}$ as well as $\text{Ca}/\text{SO}_4 \sim 1$.

4.2. Radium nuclides distribution in the moroccan geothermal systems

The variations of ^{226}Ra (half life of 1600 years), ^{228}Ra (5.8 years), and ^{224}Ra (3.7 days) in the Moroccan geothermal water are presented in Fig. 4. The data show predominance of ^{226}Ra over ^{228}Ra (i.e., low $^{228}\text{Ra}/^{226}\text{Ra}$ activity ratios), while the ^{224}Ra activities were consistent with ^{228}Ra (i.e., $^{224}\text{Ra}/^{228}\text{Ra}$ activity ratios ~ 1 ; Fig. 4). Previous studies have shown that Ra levels in geothermal waters are typically controlled by the temperature and salinity of the water, with warmer and saline waters have typically higher Ra activities (Sturchio et al., 2001; Vinson et al., 2013). Yet our data show that both temperature and salinity only partially controlled the ^{226}Ra variations (Figs. 2 and 4c).

The distribution of ^{228}Ra and ^{226}Ra show patterns of two groups (1) geothermal waters with $^{228}\text{Ra}/^{226}\text{Ra}$ activity ratios of ~ 0.14 (Liassic rocks of the High Atlas Mountain); and (2) geothermal water with lower $^{228}\text{Ra}/^{226}\text{Ra}$ activity ratios of ~ 0.04 (geothermal from the Rif area and one site associated with granitic rocks; Fig. 4). In both cases, the low $^{228}\text{Ra}/^{226}\text{Ra}$ activity ratios could indicate (1) slow-rate rock dissolution that resulted in decay of the short-lived ^{228}Ra nuclide; and (2) Ra mobilization from rocks via alpha recoil characterized by predominance of uranium (source of ^{226}Ra) over thorium (source of ^{228}Ra). If dissolution were the mechanism for Ra mobilization, the levels of the short-live ^{224}Ra would be negligible. Yet the $^{224}\text{Ra}/^{228}\text{Ra}$ activity ratios close to unity indicate that Ra is mobilized through alpha-recoil process, rather than dissolution process. The apparent secular equilibrium of ^{224}Ra with its grandparent nuclide ^{228}Ra suggests that continuously recoil of these elements from the aquifer rocks, which control the distribution of Ra nuclides in the geothermal waters. Consequently, the low

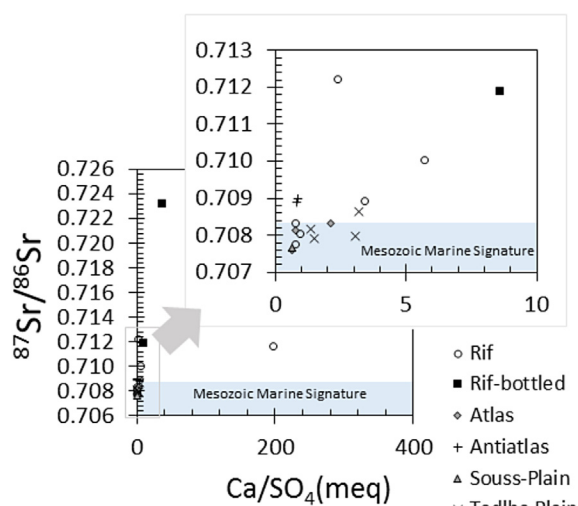


Fig. 7. $^{87}\text{Sr}/^{86}\text{Sr}$ ratios versus Ca/SO_4 ratios geothermal waters from Morocco sorted by their geographic location. The data show that geothermal waters low $^{87}\text{Sr}/^{86}\text{Sr}$ correspond to Ca/SO_4 ratios \sim unity that reflects direct dissolution of marine sulfate minerals. The increase of $^{87}\text{Sr}/^{86}\text{Sr}$ is associated with an increase of Ca/SO_4 ratios, reflecting contribution of other source rocks, presumably marine clays with radiogenic $^{87}\text{Sr}/^{86}\text{Sr}$ ratios.

$^{228}\text{Ra}/^{226}\text{Ra}$ activity ratios in the geothermal waters (Fig. 4) reflect the rock composition with predominance of uranium over thorium, rather than the rate of water-rock interactions. Since uranium is predominant in both granitic and carbonate rocks, we see only a small difference in the $^{228}\text{Ra}/^{226}\text{Ra}$ ratios in geothermal waters from carbonate/sulfate versus granitic rocks.

The absolute concentrations of radium nuclides exceed in some sites the EU drinking water threshold levels (1 Bq/L for ^{226}Ra ; 0.1 Bq/L for ^{228}Ra), particularly for sites #11, 13, and 14. The U.S. EPA drinking water regulations are more restrictive, with an upper limit for combined ^{226}Ra and ^{228}Ra (0.185 Bq/L). Combined ^{228}Ra and ^{226}Ra levels in a fraction of the Moroccan geothermal water exceeded the U.S. EPA threshold level.

4.3. Implications for water utilization

In order to evaluate the link between water quality and water use of the geothermal waters from Morocco we integrated the water quality data (Table 2) with the water use, specified in Table 1 for each site. We sorted the geothermal water by its use; geothermal waters that are used for spa recreation only, spa combined with sporadic drinking water, and regular drinking water and irrigation utilization. The variations of chloride, sulfate, TDS, and combined $^{226}\text{Ra} + ^{228}\text{Ra}$ activities in the Moroccan geothermal water sorted by water use are presented in Fig. 8. The data show that the saline geothermal waters (4000 to 16,000 mg/L; sites #1, 3, 5–7, 11) are characterized by chloride and sulfate levels above the secondary drinking water regulations (both 250 mg/L). Likewise, sodium concentrations and the calculated Sodium Absorption Ratio (SAR) values are high (a range of 3–220), which pose risks for soil stability when these waters are used for irrigation. Geothermal waters with lower concentrations of TDS (1800–3500 mg/L; sites #2, 9, 12, 13, 14) have much lower Cl and Na concentrations but high sulfate concentration (except site #9 with high alkalinity). The sulfate levels (1200 to 1900 mg/L) exceed the Secondary drinking water regulations U.S. (250 mg/L). The World Health Organization (WHO, 2004) did not include sulfate in the health-based guidelines for drinking water, but nonetheless showed cases for laxative effects in populations using drinking water with sulfate > 1000 mg/L. Geothermal water samples with low TDS (600–1400 mg/L; sites #4, 8, 10, 15, 16, 17, 18, 19, 20, 21, 22) also contained low concentrations of other dissolved constituents below any drinking water standard. In particular, geothermal waters that are used for irrigation had low boron contents (Table 2) below 1 ppm that could cause plant toxicity. Likewise, all the geothermal waters had low uranium contents (up to 3 $\mu\text{g}/\text{L}$ Table 2), an order of magnitude below the international drinking water standards (e.g., U.S. EPA of 30 $\mu\text{g}/\text{L}$).

Overall, the data show that several geothermal waters that are used for both spa and sporadic drinking water have chloride and sulfate levels above the Secondary drinking water limit, and in some cases also above 1000 mg/L of sulfate that can cause laxative effects. Yet most of the geothermal waters that are used for regular drinking water and irrigation have chloride and sulfate levels below the Secondary drinking water limit. In contrast, the $^{226}\text{Ra} + ^{228}\text{Ra}$ activity levels exceeded the U.S. EPA drinking water standard of 0.185 Bq/L in several geothermal waters that are used for both regular and sporadic drinking water, irrigation, and spas (Fig. 8). In particular, geothermal waters from sites #9, 13, and 14 had high $^{226}\text{Ra} + ^{228}\text{Ra}$ activities (0.8–0.9 Bq/L) and sites from 2, 19, 20, and 21 had lower levels (0.20–0.26 Bq/L) above the threshold value of 0.185 Bq/L. These radiation levels should be considered so as to avoid direct supply of these geothermal waters to the domestic sector, but instead could be used when blended with other water sources to mitigate the radium effect.

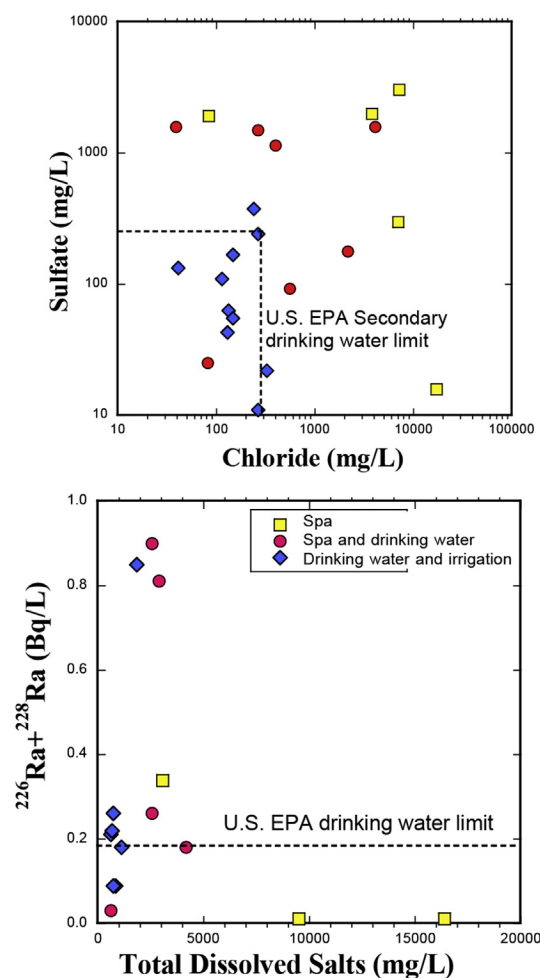


Fig. 8. Variations of TDS, chloride, sulfate, and $^{226}\text{Ra}+^{228}\text{Ra}$ (in Bq/L) concentrations in geothermal waters from Morocco, sorted by water use. The geothermal waters are used for recreation (spa) [yellow rectangles], recreation (spa) and sporadic drinking water [red circles], and for regular drinking water and irrigation [blue diamonds]. The data show that many saline geothermal waters have chloride and sulfate levels above the U.S. EPA Secondary drinking water standards and some even above sulfate contents of 1000 mg/L that, according to the WHO, can cause laxative effects. Some of the sites that are used for drinking water (both sporadic and regular use) have combined $^{226}\text{Ra}+^{228}\text{Ra}$ activities above the U.S. EPA drinking water standard of 0.185 Bq/L that could pose human health risk upon long-term utilization. (For interpretation of the references to colour in this figure legend, the reader is referred to the web version of this article.)

5. Conclusion

This study reveals the sources of solutes in geothermal waters from Morocco. Integration of multiple isotope tracers indicate the most of the Moroccan geothermal waters originated from meteoric water recharge combined with water-rock interaction. While most of the geothermal waters (as springs and boreholes) flow through carbonate rocks, the data show that dissolution of marine evaporite rocks (halite and gypsum/anhydrite) is the principle source of solutes that control the chemistry and the salinity of the geothermal waters. The strontium and boron isotope data are useful to delineate the relative contribution of marine carbonate/sulfate rocks, Sr isotopic ratios close to the secular $^{87}\text{Sr}/^{86}\text{Sr}$ variations of seawater, relative to contributions from clay minerals and shale rocks, with high (radiogenic) $^{87}\text{Sr}/^{86}\text{Sr}$ and $\delta^{11}\text{B}$. Radium isotopes indicate that Ra is mobilized from alpha-recoil of parent nuclides on the host rocks with low $^{228}\text{Ra}/^{226}\text{Ra}$ ratios that mimic

the low Th/U ratios in the rocks. Water quality and radioactivity in Morocco showed three types of geothermal waters; highly saline with high concentrations of chloride and sodium, brackish with high sulfate and radium activities, and low-saline waters typically with high quality. The highly saline geothermal water should not be used for the domestic or agricultural sectors without adequate treatment. The brackish waters that are used sporadically for drinking could pose some health effects due to high levels of sulfate and radium. The relatively low salinity waters can be used for both irrigation and drinking, although we have identified several sites with marginal high radium that should be addressed by treatment or blending prior to any utilization for the domestic sector. Nonetheless, all of the geothermal waters can be used for the tourist industry as part of spa development, particularly in the High Atlas region.

Acknowledgements

This study was supported from the Science for Peace program in NATO (Project ESP.MD.SFPP 983134). We thank the Hydraulic Agency of Souss-Massa basin for their help throughout the project. The study also benefited in part from funds allocated by the IAEA through both CRP projects (MOR16166 and 17199). We thank two anonymous reviewers and the editor for highly constructive and detailed comments that improved the quality of an early version of this paper.

References

- Bouchaou, L., Michelot, J.L., Vengosh, A., Hsissou, Y., Qurtobi, M., Gaye, C.B., Bullen, T.D., Zuppi, G.M., 2008. Application of multiple isotopic and geochemical tracers for investigation of recharge, salinization, and residence time of water in the Souss-Massa aquifer, Southwest of Morocco. *J. Hydrol.* 352, 267–287.
- Bouchaou, L., Qurtobi, M., Michelot, J.L., Zine, N., Gaye, C.B., Aggarwal, P.K., Marah, H., Zerouali, A., Taleb, H., Vengosh, A., 2009. Origin and residence time of the groundwater in the Tadla basin (Morocco) using multiple isotopic and chemical tools. *J. Hydrol.* 379, 323–338.
- Bouchaou, L., Tagma, T., Michelot, J.L., Boutaleb, S., Massault, M., Hsissou, Y., Bouragba, L., Elfaskaoui, M., 2013. Isotopic Tracers to Study Relationship between Surface Water and Groundwater: Case of Souss Upstream Catchment (Morocco). *TECDOC, IAEA, Vienna, Austria.*
- Burke, W.H., Denison, R.E., Hetherington, E.A., Koepnick, R.B., Nelson, H.F., Otto, J.B., 1982. Variation of seawater $^{87}\text{Sr}/^{86}\text{Sr}$ throughout Phanerozoic time. *Geology* 10, 516–519.
- Castorina, F., Di Biasio, E., Masp, U., Tolomeo, L., 1999. Strontium isotope evidence for the origin of barite from four mineralisations of the Moroccan Meseta. *J. Afr. Earth Sci.* 29 (3), 619–625.
- Cidu, R., Bahaj, S., 2000. Geochemistry of thermal waters from Morocco. *Geothermics* 29, 407–430.
- Clark, I., Fritz, P., 1997. *Environmental Isotopes in Hydrogeology*. Lewis Publishers, Boca Raton, USA.
- Craig, H., 1961. Isotopic variations in meteoric waters. *Science* 133, 1702–1703.
- Dansgaard, W., 1964. Stable isotopes in precipitation. *Tellus* 16, 436–468.
- Dupalova, T., Sracek, O., Vencelides, Z., Zak, K., 2012. The origin of thermal waters in the northeastern part of the eger rift, Czech Republic. *Appl. Geochem.* 27, 689–702.
- Dwyer, G., Vengosh, A., 2008. Alternative Filament Loading Solution for Accurate Analysis of Boron Isotopes by Negative Thermal Ionization Mass Spectrometry. *American Geophysical Union, Fall Meeting 2008.*
- El Morabitii, K., Ceron, J.-C., Pulido-Bosch, A., Ben Makhlof, M., Chalouan, A., El Hajjaji, K., 1998. Consideraciones sobre las aguas termales de la region de Rharb-Sais (Marruecos). *Geogaceta* 23, 35–38.
- Ettayfi, N., Bouchaou, L., Michelot, J.L., Tagma, T., Warner, N., Boutaleb, S., Massault, M., Lgourna, Z., Vengosh, A., 2012. Geochemical and isotopic (oxygen, hydrogen, carbon, strontium) constraints for the origin, salinity, and residence time of groundwater from a carbonate aquifer in the Western Anti-Atlas Mountains, Morocco. *J. Hydrol.* 438–439, 97–111.
- Favara, R., Grassa, F., Inguaggiato, S., Valenza, M., 2001. Hydrogeochemistry and stable isotopes of thermal springs: earthquake-related chemical changes along Belice Fault Western Sicily. *Appl. Geochem.* 16, 1–17.
- Hakam, O.K., Choukri, A., Reyss, J.L., Lferde, M., 2001. Determination and comparison of Uranium and Radium isotopes activities and activity ratios in samples from some natural water sources in Morocco. *J. Environ. Radioact.* 57, 175–189.
- Hakam, O.K., Choukri, A., Abbad, A., Elharfi, A., 2015. Uranium and radium activities measurements and calculation of effective doses in some drinking water samples in Morocco. *Int. J. Cancer Ther. Oncol.* 3 (3), 332.

- Lahrach, A., Zarhoulou, Y., Ben Aabidate, L., Bour, S., Ben Dhia, H., Khattach, D., Boughriba, M., El Mandour, A., Jebrane, R., 1998. Géochimie des eaux chaudes et prospection géothermique de surface au Maroc septentrional : caractérisation du réservoir d'origine et indices thermiques. *Hydrogéologie* 3, 3–19.
- Loges, A., Wagner, Th., Kirnbauer, Th., Göb, S., Bau, M., Berner, Z., Markl, G., 2012. Source and origin of active and fossil thermal spring systems, northern Upper Rhine Graben, Germany. *Appl. Geochem.* 27, 1153–1169.
- Marques, J.M., Andrade, M., Carreira, P.M., Eggenkamp, H.G.M., Graça, R.C., Aires-Barros, L., Antunes da Silva, M., 2006. Chemical and isotopic signatures of HCO₃/Na/CO₂-rich geofluids, North Portugal. *Geofluids* 6, 273–287.
- Marques, J.M., Carreira, P.M., Goff, F., Eggenkamp, H.G.M., Antunes da Silva, M., 2012. Input of ⁸⁷Sr/⁸⁶Sr ratios and Sr geochemical signatures to update knowledge on thermal and mineral waters flow paths in fractured rocks (N-Portugal). *Appl. Geochem.* 27, 1471–1481.
- Nicholson, K., 1993. *Geothermal Fluids : Chemistry and Exploration Techniques*. Springer Berlin Heidelberg, Berlin, Heidelberg.
- N'da, A.B., Bouchaou, L., Reichert, B., Hanich, L., Ait Brahim, Y., Chehbouni, A., Beraaouz, E.H., Michelot, J.L., 2016. Isotopic signatures for the assessment of snow water resources in the Moroccan high Atlas Mountains: contribution to surface and groundwater recharge. *Environ. Earth Sci.* 75 (9), 1–11.
- Ouda, B., El Hamdaoui, A., Ibn Majah, M., 2004. Isotopic Composition of Precipitation at Three Moroccan Stations Influenced by Oceanic and Mediterranean Air Masses. *TECDOC 1453*. IAEA, Vienna, Austria, pp. 125–140.
- Carreira, Paula M., Marques, José M., Grac, Rui C., Barros, Luís Aires, 2008. 2008-Radiocarbon application in dating “complex” hot and cold CO₂-rich mineral water systems: a review of case studies ascribed to the northern Portugal. *Appl. Geochem.* 23, 2817–2828.
- Penna, D., Ahmad, M., Birks, S.J., Bouchaou, L., Brenčić, M., Butt, S., Holko, L., Jeelani, G., Martínez, D.E., Melikadze, G., Shanley, J., Sokratov, S.A., Stadnyk, T., Sugimoto, A., Vreča, P., 2014. A new method of snowmelt sampling for water stable isotopes. *Hydrol. Process.* 28 (22), 5637–5644.
- Raibi, F., Benkaddour, A., Hanich, L., Chehbouni, A., Chtioui, M., 2006. Variation de la composition des isotopes stables des précipitations en climat semi-aride (cas du bassin-versant de Tensift Maroc). *GIRES3D*, Marrakech, Maroc.
- Rimi A., 2000. First Assessment of Geothermal Ressources in Morocco. *Proceedings World Geothermal Congress 2000 Kyushu - Tohoku, Japan, May 28-June 10, 2000*.
- Rimi, A., Chalouan, A., Bahi, L., 1998. Heat flow in the westernmost part of the Alpine Mediterranean system (the Rif, Morocco). *Tectonophysics* 285, 135–146.
- Rimi, A., Zarhoulou, Y., Barkaoui, A.E., Correia, A., Carneiro, J., Verdoya, M., Lucazeau, F., 2012. Towards a de-carbonized energy system in north-eastern Morocco: prospective geothermal resource. *Renew. Sustain. Energy Rev.* 16, 2207–2216.
- Sosa, E., Guerra, J.C., Arenciba, M.T., 2011. Isotopic composition of rainwater in the subtropical island of Tenerife, Canary Islands. *J. Environ. Hydrol.* 19, 27.
- Sturchio, N.C., Banner, J.L., Binz, C.M., Heraty, L.B., Musgrove, M., 2001. Radium geochemistry of ground waters in Paleozoic carbonate aquifers, midcontinent, USA. *Appl. Geochem.* 16, 109–122.
- Tassi, F., Va selli, O., Moratti, G., Piccardi, L., Minissale, A., Poreda, R., Delgado Huertas, A., Bendkik, A., Chenakeb, M., Tedesco, D., 2006. Fluid geochemistry versus tectonic setting: the case study of Morocco. In: Moratti, G., Chalouan, A. (Eds.), *Tectonics of the Western Mediterranean and North Africa*, vol. 262. Geological Society, London, pp. 131–145. Special Publications.
- Veizer, J., 1989. Strontium isotopes in seawater through time. *Rev. Earth Planet. Sci.* 17, 141–167.
- Vengosh, A., Chivas, A.R., McCulloch, M.T., Starinski, A., Kolodny, Y., 1991. Boron isotope geochemistry of Australian salt lakes. *Geochim. Cosmochim. Acta* 55, 2591–2606.
- Vengosh, A., Helvácý, Karamanderesi, I.H., 2002. Geochemical constraints for origin of thermal waters from western Turkey. *Appl. Geochem.* 17, 163–183.
- Vengosh, A., Heumann, K.G., Juraske, S., Kasher, R., 1994. Boron isotope application for tracing sources of contamination in groundwater. *Environ. Sci. Technol.* 28, 1968–1974.
- Vinson, D.S., Tagma, T., Bouchaou, L., Dwyer, G.S., Warner, N.R., Vengosh, A., 2013. Occurrence and mobilization of radium in fresh to saline coastal groundwater inferred from geochemical and isotopic tracers (Sr, S, O, H, Ra, Rn). *Appl. Geochem.* 38, 161–175.
- Winckel, A., Marlin, Ch., Devera, L., Morel, J.L., Morabiti, K., Ben Makhoulouf, M., Chalouan, A., 2002. Recharge altitude estimation of thermal springs using stable isotopes in Morocco. *C. R. Geosci.* 334, 469–474.
- World Health Organization (WHO), 2004. Sulfate in Drinking-water, Background Document for Development of WHO Guidelines for Drinking-water Quality. *WHO/SDE/WSH/03.04/114*.
- Zarhoulou, Y., Lahrach, A., Ben Aabidat, L., Bour, S., Ben Dhia, H., et Khattach, D., 1998. Anomalies gbothermiques de surface et hydrodynamisme dans le bassin d'Agadir (Maroc). *J. Afr. Earth Sci.* 27 (No. 1), 71–85.
- Zarhoulou, Y., Boughriba, M., Rimi, A., Lahrach, A., 2007. Les provinces hydro-géothermiques du Maroc Potentialités et possibilités d'utilisations. Bilan sur les sources d'énergie renouvelables au Maroc. Chapitre du livre UNESCO. Les énergies renouvelables au Maroc – Le débat est lancé. UNESCO, ISBN 9954-8068-2-2, p. 164.